

ORIGINAL ARTICLE

Simulation of a parabolic trough solar collector containing hybrid nanofluid and equipped with compound turbulator to evaluate exergy efficacy and thermal-hydraulic performance

Yacine Khetib^{1,2} | Ahmad Alahmadi³  | Ali Alzaed⁴ | Mohsen Sharifpur^{5,6} | Goshtasp Cheraghian⁷  | Cornelius Siakachoma⁸ 

¹Mechanical Engineering Department, Faculty of Engineering, King Abdulaziz University, Jeddah, Saudi Arabia

²Center Excellence of Renewable Energy and Power, King Abdulaziz University, Jeddah, Saudi Arabia

³Department of Electrical Engineering, College of Engineering, Taif University, Taif, Saudi Arabia

⁴Architectural Engineering Department, Faculty of Engineering, Taif University, Taif, Saudi Arabia

⁵Department of Mechanical and Aeronautical Engineering, University of Pretoria, Pretoria, South Africa

⁶Department of Medical Research, China Medical University Hospital, China Medical University, Taichung, Taiwan

⁷Independent Researcher, Braunschweig, Germany

⁸Department of Mechanical Engineering, School of Engineering, University of Zambia, Lusaka, Zambia

Correspondence

Mohsen Sharifpur, Department of Mechanical and Aeronautical Engineering, University of Pretoria, Pretoria, South Africa.
Email: mohsen.sharifpur@up.ac.za

Cornelius Siakachoma, Department of Mechanical Engineering, School of Engineering, University of Zambia, PO Box 32379, Lusaka 10101, Zambia.
Email: csiakachoma@unza.zm

Funding information

Taif University Researchers Supporting Project; Taif University, Taif, Saudi Arabia, Grant/Award Number: TURSP-2020/121

Abstract

This research is mainly aimed at investigating the numerical modeling of thermal-hydraulic and exergy efficiencies of parabolic trough solar collectors (P-SCs) filled with magnetic hybrid nanofluid. The k-epsilon turbulence, S2S, and mixture models were used to simulate the turbulence equations, radiation, and two-phase nanofluid, respectively. The experiments were run using magnetic nanofluid in Reynolds numbers of 5000-20 000, the volume fractions of 1%-3%, and the ratios of pitch (ROPs) of 1, 2, and 3 of the combined turbulator. According to the results, there is a significant increase in average Nusselt number (Nu) and pressure drop (ΔP) with increasing Reynolds number, nano-additive concentration, and ROP. Moreover, the use of the hybrid magnetic turbulator and hybrid nanofluid increased the thermal performance of the P-SC. It was also found that the Reynolds number of 20 000 and volume fraction of 3% of nanoparticles resulted in the optimal exergy efficiency mode in using a hybrid turbulator.

KEYWORDS

compound turbulator, exergy efficiency, magnetic hybrid nanofluid, parabolic trough solar collector, PEC, two-phase flow

This is an open access article under the terms of the Creative Commons Attribution License, which permits use, distribution and reproduction in any medium, provided the original work is properly cited.

© 2021 The Authors. *Energy Science & Engineering* published by Society of Chemical Industry and John Wiley & Sons Ltd.

1 | INTRODUCTION

Given the importance of energy in everyday human life, many researchers have focused on this issue.¹⁻⁵ It has been found that renewable energy can properly meet the needs of countries. In this regard, solar energy is among the energy resources available to humans that have received considerable attention.⁶⁻¹⁰ Therefore, many studies have been conducted in this field whose results strongly recommend using renewable energy.¹¹⁻¹⁴

Recently, increasing the heat transfer rate (HTR) in renewable systems has been of interest to researchers.¹⁵⁻¹⁹ One of these methods is to use nanofluids as an alternative to conventional liquids.²⁰⁻²⁸ Nanofluids are widely used in micromixers,²⁹ heat exchangers,³⁰ and solar systems.³¹ As the experimental tests are costly,³² a very effective solution to reduce the costs and examine the effects of different parameters is to adopt numerical methods.³³⁻⁴⁰ Recently, the use of turbulators in solar collectors (SCs) to create turbulent flow and increase the resulting heat exchange has become very popular among scientists.⁴¹⁻⁴³ Ahmed et al.⁴⁴ examined the influence of using a combined generator on HTR and nanofluid flow specification within a symmetrical duct. Their work was both numerical and experimental, using two nanoparticles (Al_2O_3 and SiO_2). According to the results, using a vortex generator and nanofluid increased the HTR and ΔP . Moreover, the experimental results agreed with the numerical ones with high accuracy. Aliakbari et al.⁴⁵ investigated the impact of horizontal fibers on the flow field and HTR of alumina-water nanofluid in a microchannel utilizing the finite volume method (FVM). Their data indicated that growing the height of the ribs horizontally caused a noteworthy augmentation in HTR and ΔP . Amirahmadi et al.⁴⁶ examined the effect of a turbulator on exergy efficiency and entropy production within a trapezoidal channel using mathematical methods. Their research was conducted for Reynolds numbers of 400-1600. They found that adding the turbulator to the trapezoidal channel reduced entropy production and exergy efficiency. Sheikholeslami and Ganji⁴⁷ experimentally studied the influence of turbulators on hydrothermal efficiency of two-pipe heat exchangers for Reynolds numbers of 6000-12 000 and torsion ratios of 0.72 to 1.29. The maximum hydrothermal increase was 19.15%, which occurred at a Reynolds number of 6000 and torsion ratio of 0.72. Sheikholeslami and Ganji⁴⁸ also performed experimental and numerical studies on the effect of simple and hollow turbulators on the hydraulic performance of two-pipe converters. They used air and water fluids in the outer and inner tubes of the heat exchanger, respectively. Their findings showed that the use of hollow turbulators increased the HTR by 26.45% compared to simple turbulators. Rashidi et al.⁴⁹ numerically

investigated twisted turbulators for fluid flow performance and nanofluid entropy production within a square chamber. The study was performed at nanoparticle concentrations of 0 to 0.05, with the step ratio of the twisted turbulators varying from 180° to 540° . They found that the addition of twisted turbulators to the square chamber reduced the output of entropy. Moreover, the rise in the nanoparticles' concentration had a decreasing impact on the entropy production. Eiamsa-ard and Wongcharee⁵⁰ experimentally evaluated the impact of nonuniformly twisted tape on the thermal hydraulic output of water-Ag nanofluid in a tube. Their findings revealed that the HTR increased with the Reynolds number and nanoparticle concentration. Moreover, the placement of nonuniformly twisted tape increased the HTR by 36.21% compared to case in which the plain tube was higher. Applying numerical methods, Akbarzadeh et al.⁵¹ assessed the impact of dissimilar rib shapes on the alumina-water nanofluid behavior in a solar heater. They used triangular and semi-circular ribs with Reynolds numbers of 5000-15 000 and volume fraction of two-phase nanofluids ranging from 0% to 4%. According to the results, the index of thermal-hydraulic output in the solar heater with semicircular ribs was much higher compared to those with triangular ribs. Sharafeldin and Gró⁵² experimentally and numerically studied the impact of water-CeO₂ nanofluid on the thermal efficiency of SCs. In the experimental part of the study, they fabricated water-CeO₂ nanofluids using a two-step method. Their findings indicated that the temperature discrepancy between the inlet and outlet flow significantly increased by adding the nanofluid to the system. Furthermore, the use of water-CeO₂ nanofluid augmented the HTR by 34% in comparison with the base fluid. Bahrami et al.⁵³ employed Al_2O_3 to affect thermal behavior. With the rise in the volume fraction of the nanofluid by 4%, there was a significant improvement in the forced convection heat transfer. Applying experimental methods, Subramani et al.⁵⁴ examined the effect of water-TiO₂ nanofluid to improve efficiency and HTR in the turbulent flow regime inside the SC. The study was performed for volume fractions of 0.05%-0.5% of nanoparticles and Reynolds numbers of 2950-8142, which led to a turbulent flow regime. They reported that the thermal efficiency inside the SC increased with the Reynolds number and nanoparticle concentration. Bazdidi-Tehrani et al.⁵⁵ studied the effect of ribbed fibers on the flow field and HTR of titan-water nanofluid inside a flat plate SC. It was found that the use of ribs intensified the HTR by 10% compared to other cases. Furthermore, increasing the concentration of nanoparticles resulted in an increment in the thermal efficacy of the flat panel SC. Nguyen et al.⁵⁶ applied a triangular rib to make turbulence by exerting magnetic particles. They reported that the simultaneous

effect of triangular rib and magnetic nanoparticle could boost the heat transfer by 25%. Obaid et al.⁵⁷ checked the influence of a new turbulator on the thermal-economic performance of SCs. It was found that by creating a vortex and disrupting the thermal layers, using new turbulators brought about a remarkable increment in the thermal performance of the SC. The new turbulators were also economically viable. Singh et al.⁵⁸ examined the impression of different ribs on the outputs of a solar heater applying a kinematic method. They claimed that when using circular and trapezoidal ribs, the thermal output of the solar heater grew by 17% and 16%, respectively. Employing numerical methods, Ekiciler et al.⁵⁹ evaluated the influence of hybrid nanofluids on the thermal performance in a P-SC. Their study was performed on Syltherm 800-based hybrid nanofluids at nanoparticle concentrations of 1%-4%. It was found that the thermal output of the P-SC increased with the nanoparticles' concentration. Sheikholeslami and Farshad⁶⁰ numerically investigated the impact of innovative turbulators on the thermal performance within a SC. Their findings revealed that the addition of light turbulators enhanced the SC thermal performance by 56.04% in comparison with the case when the SC had no turbulator.

The following is the innovations of the present work:

1. The use of a magnetic hybrid nanofluid
2. The use of innovative hybrid turbulators
3. Exergy study in parabolic solar collectors

A review of the literature reveals that the thermal-hydraulic performance and exergy efficacy of the parabolic trough solar collectors (P-SC) equipped with new hybrid turbulators filled with a water-Fe₃O₄-MWCNT

hybrid nanofluid have not been studied so far, considering the two-phase model in a turbulent flow. Accordingly, the present study has investigated the effect of a hybrid turbulator for the pitch ratios (PRs) of 1, 2, and 3 at Reynolds numbers of 5000-20 000 and volume fractions of 1%-3% of two-phase hybrid nanofluid using mathematical methods.

2 | NUMERICAL INSTRUCTION

2.1 | Physical model

Figure 1 demonstrates a schematic of the investigated P-SC. As can be seen, the SC was equipped with a compound turbulator. The length of the solar culture was 700 mm, the length of the hybrid turbulator was 200 mm, and the diameter of the absorber tube was 50 mm. According to the figure, three different torsion ratios of 1, 2, and 3 for the combined turbulator were studied. The inputs of the study were Reynolds numbers of 5000-20 000, with the volume fractions of the two-phase hybrid nanofluid ranging from 1% to 3%.

2.2 | Governing equations

In order to simulate the MWCNT-Fe₃O₄/water magnetic hybrid nanofluid flow through the P-SC, a mixed two-phase liquid model was applied, which is more accurate compared with other methods.⁶¹ In all models simulated during the present investigation, the fluid flow inside the P-SC was turbulent because the Reynolds number was over 2300. Due to the simulation of the turbulent flow inside the absorber tube, the equations of the k - ϵ model

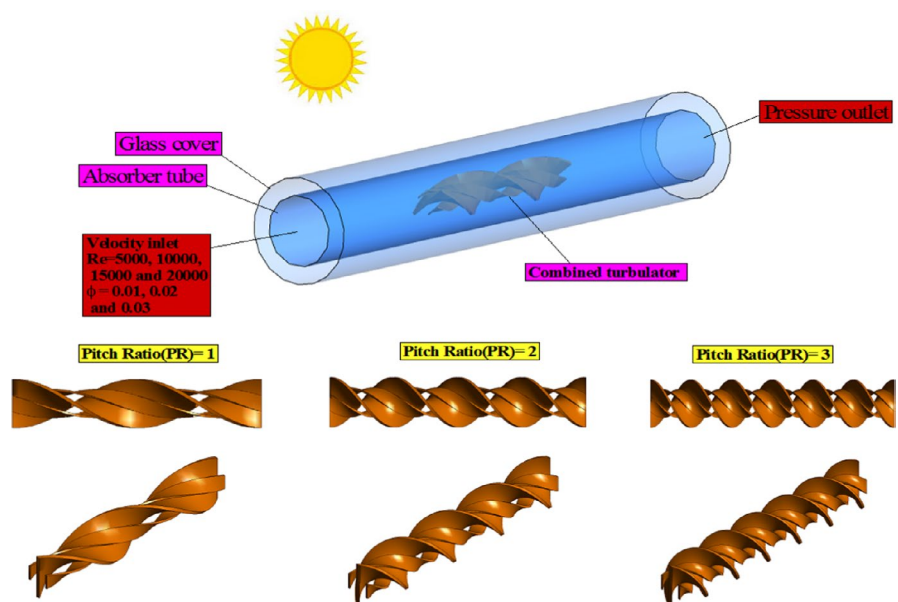


FIGURE 1 A schematic of the studied P-SC with the compound turbulator

were used, as well as the equations of continuity, motion, and energy, in the commercial software ANSYS-Fluent. The following provides the equations used^{62,63}:

Continuity equation:

$$\frac{1}{r} \frac{\partial}{\partial \theta} (\rho u) + \frac{1}{r} \frac{\partial}{\partial r} (\rho r v) + \frac{\partial}{\partial z} (\rho w) = 0. \quad (1)$$

Momentum equations:

$$\begin{aligned} \frac{1}{r} \frac{\partial}{\partial \theta} (\rho u u) + \frac{1}{r} \frac{\partial}{\partial r} (\rho r v u) + \frac{\partial}{\partial z} (\rho w u) + \frac{1}{r} (\rho u v) = \\ -\frac{1}{r} \frac{\partial P}{\partial \theta} + \frac{1}{r^2} \frac{\partial}{\partial \theta} \left(\mu \frac{\partial u}{\partial \theta} \right) + \frac{\partial}{\partial r} \left(\mu \frac{1}{r} \frac{\partial}{\partial r} (r u) \right) + 2\mu \frac{1}{r^2} \frac{\partial v}{\partial \theta} + \rho g \beta (T_w - T) \sin \theta, \end{aligned} \quad (2)$$

$$\begin{aligned} \frac{1}{r} \frac{\partial}{\partial \theta} (\rho u v) + \frac{1}{r} \frac{\partial}{\partial r} (\rho r v v) + \frac{\partial}{\partial z} (\rho w v) - \frac{1}{r} (\rho u^2) = \\ -\frac{1}{r} \frac{\partial P}{\partial \theta} + \frac{1}{r^2} \frac{\partial}{\partial \theta} \left(\mu \frac{\partial v}{\partial \theta} \right) + \frac{\partial}{\partial r} \left(\mu \frac{1}{r} \frac{\partial}{\partial r} (r v) \right) - 2\mu \frac{1}{r^2} \frac{\partial u}{\partial \theta} - \rho g \beta (T_w - T) \cos \theta, \end{aligned} \quad (3)$$

$$\frac{1}{r} \frac{\partial}{\partial \theta} (\rho u w) + \frac{1}{r} \frac{\partial}{\partial r} (\rho r v w) + \frac{\partial}{\partial z} (\rho w w) = -\frac{\partial P}{\partial z} + \frac{1}{r^2} \frac{\partial}{\partial \theta} \left(\mu \frac{\partial w}{\partial \theta} \right) + \frac{1}{r} \frac{\partial}{\partial r} \left(r \mu \frac{\partial w}{\partial r} \right), \quad (4)$$

where r , θ , and z are the coordinates, and u , v , and w are the velocity components.

Energy equation:

$$\begin{aligned} \frac{1}{r} \frac{\partial}{\partial \theta} (\rho u T) + \frac{1}{r} \frac{\partial}{\partial r} (\rho r v T) + \frac{\partial}{\partial z} (\rho w T) = \\ \frac{1}{r^2} \frac{\partial}{\partial \theta} \left(\frac{k}{c_p} \frac{\partial T}{\partial \theta} \right) + \frac{1}{r} \frac{\partial}{\partial r} \left(r \frac{k}{c_p} \frac{\partial T}{\partial r} \right). \end{aligned} \quad (5)$$

As noted previously, the Reynolds number is defined as⁶²:

$$\text{Re} = \frac{\rho_f \cdot u_m \cdot D_i}{\mu_f}. \quad (6)$$

The average Nu is expressed as⁶²:

$$\text{Nu} = \frac{h_f \cdot D_i}{k_f}. \quad (7)$$

The following equation gives the pressure drop:

$$\Delta P = P_{av,inlet} - P_{av,outlet}. \quad (8)$$

Further, the friction factor coefficient is computed as⁶³:

$$f = \frac{2}{\left(\frac{L}{D_i}\right)} \frac{\Delta P}{\rho_{nf} \cdot u_m^2}. \quad (9)$$

The thermal and hydraulic performance evaluation criterion (PEC) can be defined as the following equation to make a comparison between the hydrothermal performance of simple P-SC and compound turbulator⁶²:

$$\text{PEC} = \left(\frac{Nu_{av}}{Nu_{av,0}} \right) \cdot \left(\frac{f}{f_0} \right)^{-1/3}. \quad (10)$$

The exergy efficiency for parabolic collectors is expressed as the net useful exergy divided by the exergy of direct solar radiation entering the collector and is calculated using the following equation:

$$\eta_{ex} = \frac{\dot{Q}_{HTF} - \dot{m}_{HTF} C_{p,HTF} \ln \left(\frac{T_{\infty}}{T_{i,HTF}} \right)}{\dot{Q}_{HTF} - \dot{m}_{BF} C_{p,BF} \ln \left(\frac{T_{0,BF}}{T_{i,BF}} \right) + VI_{\eta P}}, \quad (11)$$

in which, η_P is the pump power, which was considered equal to 85%.

2.3 | Nanofluid

The Newtonian nanofluid, called magnetic hybrid nanofluid, was used in the current study. It was comprised of water, Fe_3O_4 , and MWCNT, and applied in the two-phase mixture method for simulation. The volume fraction varied from 0.01 to 0.03. Table 1 lists the properties of the thermophysical nanofluid.

As the hybrid nanofluid included various materials, the density of water- Fe_3O_4 -MWCNT nanofluid (ρ_{nf}) could be obtained as follows:^{64,65}

$$\rho_{nf} = \rho_{np1} \varphi_{np1} + \rho_{np2} \varphi_{np2} + \rho_f (1 - \varphi_{np1} - \varphi_{np2}), \quad (12)$$

and the specific heat, $c_{p,nf}$, of this hybrid nanofluid is obtained from the following equation:

$$\begin{aligned} (\rho c_p)_{nf} = (\rho c_p)_{np1} \varphi_{np1} + (\rho c_p)_{np2} \varphi_{np2} \\ + (\rho c_p)_f (1 - \varphi_{np1} - \varphi_{np2}). \end{aligned} \quad (13)$$

Furthermore, the thermal conductivity and dynamic viscosity of the aforementioned nanofluid can be described as conformity relations^{64,65}.

$$k_{nf} = k_f \left(\frac{(k_{np1} + k_{np2}) + 2k_f - 2\varphi_{np1}(k_f + k_{np1}) - 2\varphi_{np2}(k_f + k_{np2})}{(k_{np1} + k_{np2}) + 2k_f - \varphi_{np1}(k_f + k_{np1}) - \varphi_{np2}(k_f + k_{np2})} \right), \quad (14)$$

$$\mu_{nf} = \mu_f(1 - \phi_1 - \phi_2)^{-2.5}. \quad (15)$$

It should be mentioned that ϕ is a parameter to change the volume concentration of Fe_3O_4 -MWCNT nanoparticles.

2.4 | Validation

2.4.1 | Grid independency testing

In order to obtain a proper grid, the mean Nu was evaluated for various grids in a P-SC with ROP = 3 at $\text{Re} = 20\,000$ and $\phi = 3\%$ (see Table 2). According to the values of the mean Nu, it was observed that the grids with a number of 1 391 674 were suitable for simulating the P-SC with ROP = 3

2.4.2 | Numerical procedure validation

The numerical results were validated with the results of a study by He et al.⁶⁶ Based on the outputs of Figure 2, the discrepancy of the mean Nu values obtained in the simulations was small compared to that obtained by He et al.,⁶⁶ and the maximum error rate was 4.78%. As an outcome, the precision of the modeling results was ensured.

TABLE 1 The properties of the thermophysical nanofluid at $T = 300\text{ K}$ ^{64,65}

Material	$\rho(\text{kg/m}^3)$	$c_p(\text{J/kg K})$	$k(\text{W/m K})$	$\mu(\text{N}\cdot\text{s/m}^2)$
Water	998.2	4182	0.6	0.001003
Fe_3O_4	5200	670	6	-
MWCNT	2100	519	3000	-

TABLE 2 Average Nu for water- Fe_3O_4 -MWCNT magnetic hybrid nanofluid inside P-SC with ROP = 3, for $\text{Re} = 20\,000$, and $\phi = 0.03$

Grid	Eodes	Nu_{ave}	Relative error (%)
1	534 945	410.91	-
2	874 581	489.67	19.17
3	1 019 892	516.31	5.44
4	1 391 674	517.80	0.29
5	1 649 371	517.97	0.03

3 | RESULTS AND DISCUSSION

This section provides the outcomes of the numerical simulation. First, the pressure, speed, and temperature of the

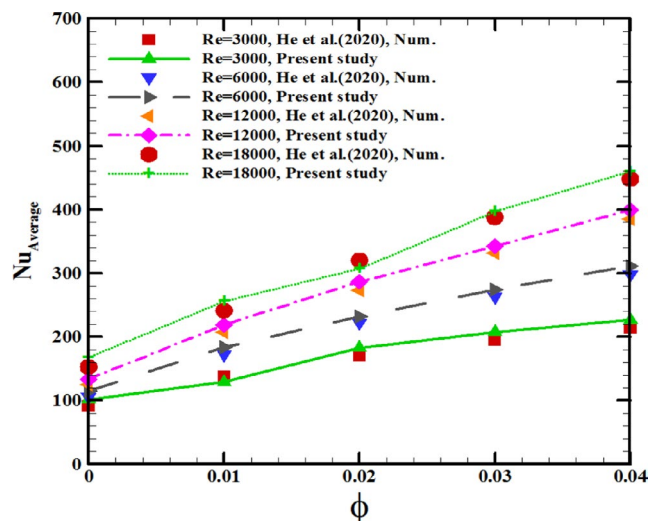


FIGURE 2 Outcomes of the numerical validation with He et al.⁶⁶

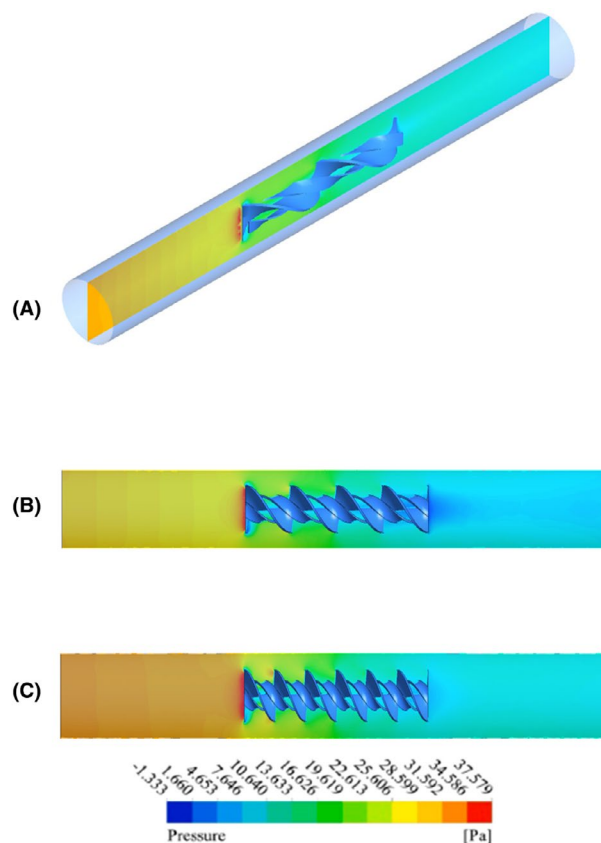


FIGURE 3 Pressure contours for $\text{Re} = 20\,000$ and in P-SC for (A) ROP = 1, (B) ROP = 2, and (C) ROP = 3

P-SC are given. Then, the diagrams of changes in mean Nu, ΔP , PEC index, and exergy efficiency changes are presented.

Figure 3 shows the pressure-related contours for $Re = 20\,000$ and in the P-SC for different ROPs. Based on the pressure meters, it is clear that the density of flow lines for a P-SC with $ROP = 3$ (c) was much higher compared to $ROP = 1$ (a) and $ROP = 2$ (b). This can be attributed to the change in torsion ratio, the flow between the blades, and the twists of the compound turbulator, causing the accumulation of lines. The pressure also decreased with the increasing length of the P-SC. In all P-SCs, the pressure was maximum at the inlet of the channel. The inactive flow caused a lot of pressure at the inlet due to the collision with the compound turbulator; and as a result, the whole speed changes to pressure.

Figure 4 shows the velocity contours for $Re = 20\,000$ and the P-SC for different ROPs. As can be seen, in the P-SC close to the walls, since there was no slip, it stuck to the collector walls, and its speed was equal to the speed on the wall. Therefore, near the P-SC wall, the velocity had its lowest value. However, by approaching the center of the P-SC, the speed increased over time. Separation

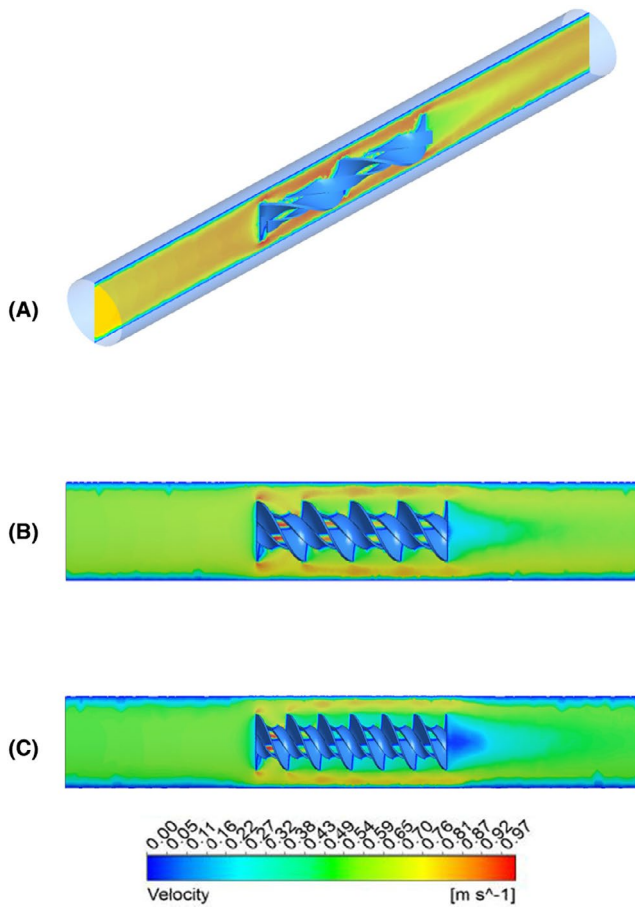


FIGURE 4 Speed contours for $Re = 20\,000$ in the P-SC for (A) $ROP = 1$, (B) $ROP = 2$, and (C) $ROP = 3$

occurred when the current struck the hybrid turbulators, which formed the vortices and made them swirl. As can be seen, the size of these vortices in the parabolic collector with $ROP = 3$ was much larger and more elongated compared to the combined turbulator with $ROP = 1$ and $ROP = 2$.

Figure 5 shows the pressure contours for $Re = 20\,000$ in the P-SC for different ROPs. The figure for the thermal boundary layer increased with the ROP. The existence of vortices was the reason behind this phenomenon.

Figure 6 shows the changes in flow lines for $Re = 20\,000$ in the P-SC for different ROPs. As can be seen, the density of flow lines increased with the ROP. However, the highest density of flow lines belonged to the P-SC with a hybrid turbulator of $ROP = 3$.

Figure 7 depicts the average Nu changes against the Reynolds number in the P-SC with turbulator in different ROPs and volume fractions. As can be seen, the average Nu grew with the Reynolds number. It can be said that the velocity and density of the flow lines increased with the Reynolds number, resulting in a higher heat transfer coefficient. Furthermore, the rise in the ROP in the P-SC

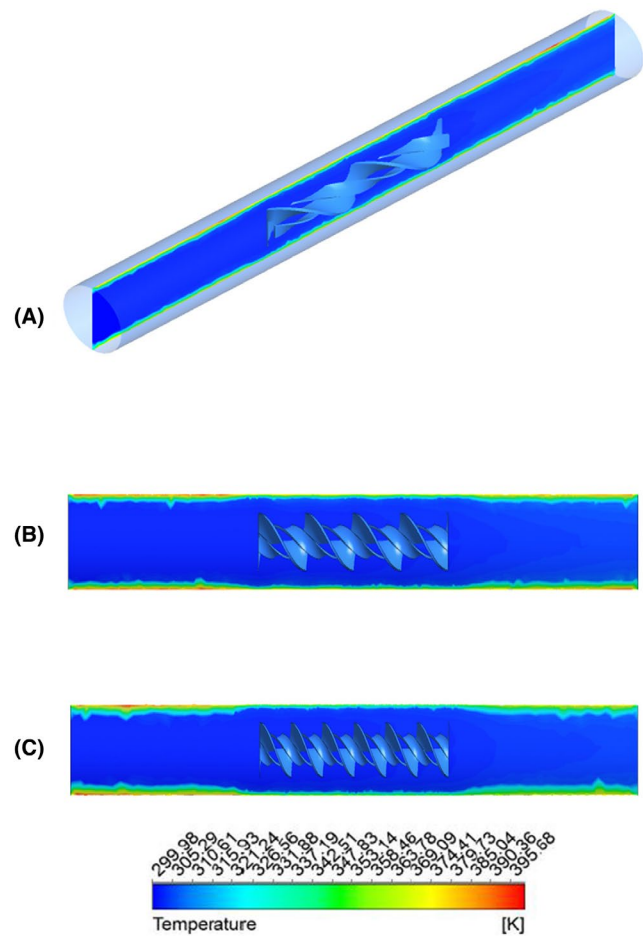


FIGURE 5 Temperature contours for $Re = 20\,000$ in P-SC for (A) $ROP = 1$, (B) $ROP = 2$, and (C) $ROP = 3$

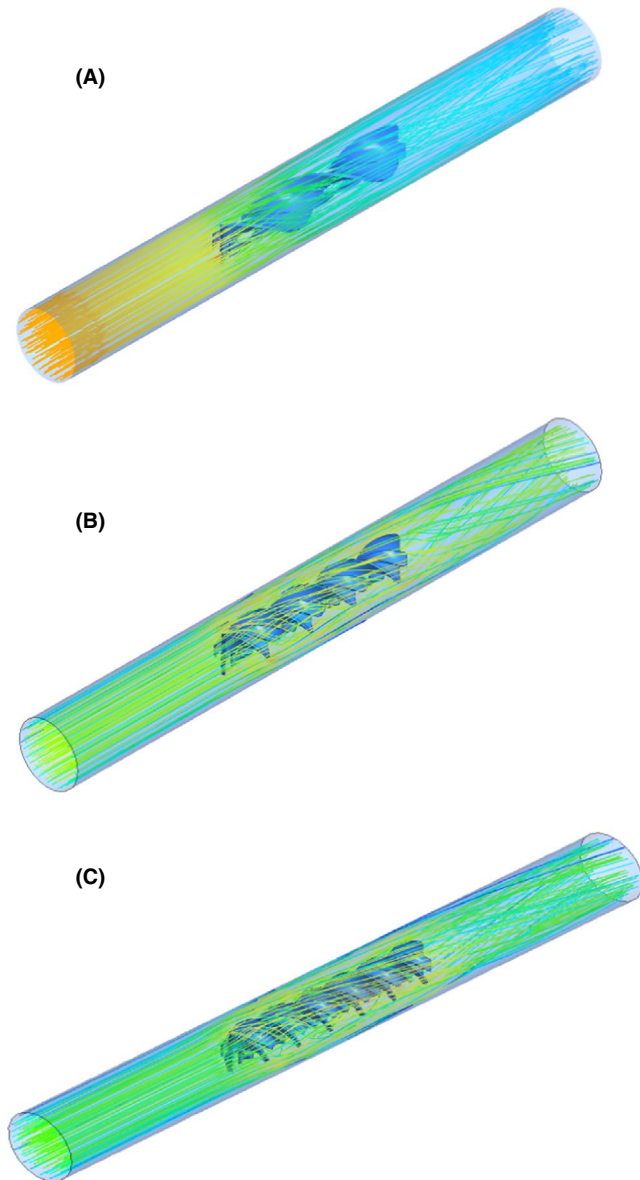


FIGURE 6 Streamline changes for $Re = 20\,000$ in P-SC for (A) $ROP = 1$, (B) $ROP = 2$, and (C) $ROP = 3$

increases the thermal performance, significantly. This can be attributed to the increased mixing and turbulence. For this reason, the average Nu would increase as a representative of this HTR. The rise in the average Nu in SC with $ROP = 3$ was more than the other two cases, which can be attributed to the presence of more vortices. These vortices, as shown in the contours in the previous section, were longer and longer when the combined turbulator was longer. Therefore, their accumulation between the blades and the twists of the combined turbulator would increase the HTR. The maximum increase in thermal performance belonged to $ROP = 3$ and a volume fraction of 3% of nanoparticles. At Reynolds numbers of 5000, 10 000, 15 000, and 20 000, it increased by 70.93%, 81.16%, 70.63%, and 56.10%, respectively.

Figure 8 demonstrates the variations in ΔP against Reynolds number in a P-SC with turbulator in different ROP ratios and volume fractions. As can be seen, the ΔP was greater when the P-SC with $ROP = 3$ was larger than the two ROP channels. Therefore, the pressure increased with an increase in the ROP in the hybrid turbulator. The maximum increase in ΔP was associated with $ROP = 3$ and a volume fraction of 3% of nanoparticles. At Reynolds numbers of 5000, 10 000, 15 000, and 20 000, it increased by 19.53%, 110.28%, 100.22%, and 80.23%, respectively.

Figure 9 presents the changes of PEC index to Reynolds number in volume fraction of 1%-3% of nanoparticles in P-SC with combined turbulator for $ROP = 1$ (a), $ROP = 2$ (b), and $ROP = 3$ (c), respectively. As can be seen, the PEC index in the P-SC with hybrid turbulator was higher than 1 for all volume fractions and ROPs. Therefore, these results showed that the use of hybrid state turbulators had an effective role in improving HTR, and its use in a P-SC was appropriate in terms of the PEC index.

Exergy performance discrepancy against Reynolds number in a P-SC with a combined turbulator for $ROP = 1, 2, \text{ and } 3$ at various volume fractions is depicted in Figure 10. As it is demonstrated, in all cases, the exergy performance grew with the volume fraction. However, in all cases, exergy efficiency increased with rising Reynolds number until reaching 10 000, and then decreased. Therefore, it can be concluded that the optimal state of exergy occurred in Reynolds number of 10 000 and volume fraction of 0.03% of nanoparticles.

4 | CONCLUSION

In this study, the effect of a hybrid turbulator with the pitch ratios of 1, 2, and 3, Reynolds numbers of 5000-20 000, and volume fractions of 1%-3% of two-phase hybrid nanofluid was evaluated through mathematical methods. Based on numerical methods, the impact of compound turbulator on thermal-hydraulic performance and exergy efficiency of P-SC filled with magnetic hybrid nanofluid and modeled in two phases was examined. The use of compound turbulators and magnetic hybrid nanofluids boosted the thermal performance of the P-SC. The maximum increase in ΔP belonged to $ROP = 3$ and volume fraction of 3% of nanoparticles. At Reynolds numbers of 5000, 10 000, 15 000, and 20 000, it increased by 19.53%, 110.28%, 100.22%, and 80.23%, respectively. The use of hybrid turbulators in terms of the PEC index in P-SC was desirable. The optimal mode of using a hybrid turbulator in terms of exergy efficiency belonged to Reynolds number of 20 000 and volume fraction of 3% of nanoparticles.

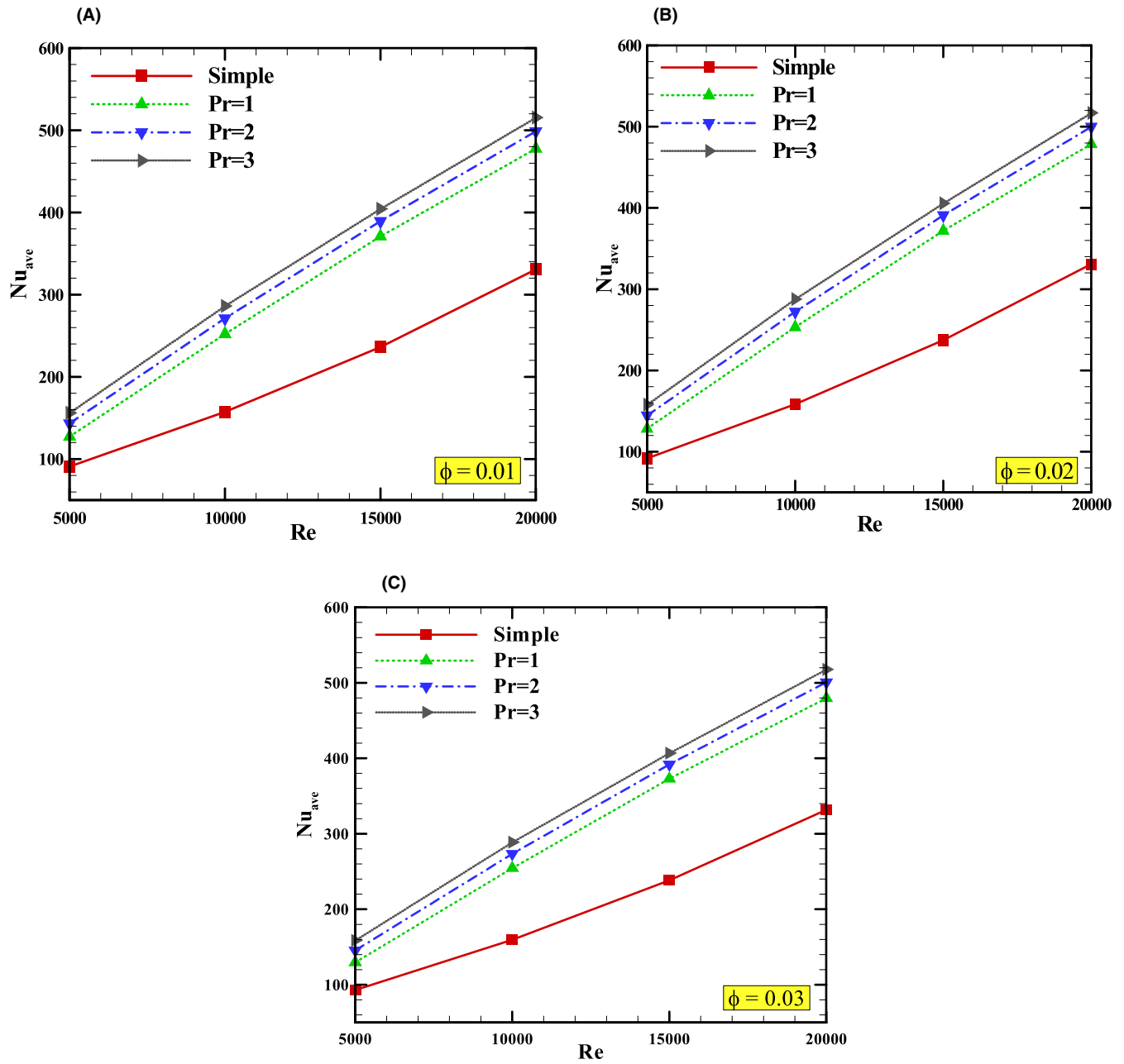


FIGURE 7 Variation of average Nu against Re number in P-SC with combined turbulator in different ROPs for (A) $\phi = 0.01$, (B) $\phi = 0.02$, and (C) $\phi = 0.03$

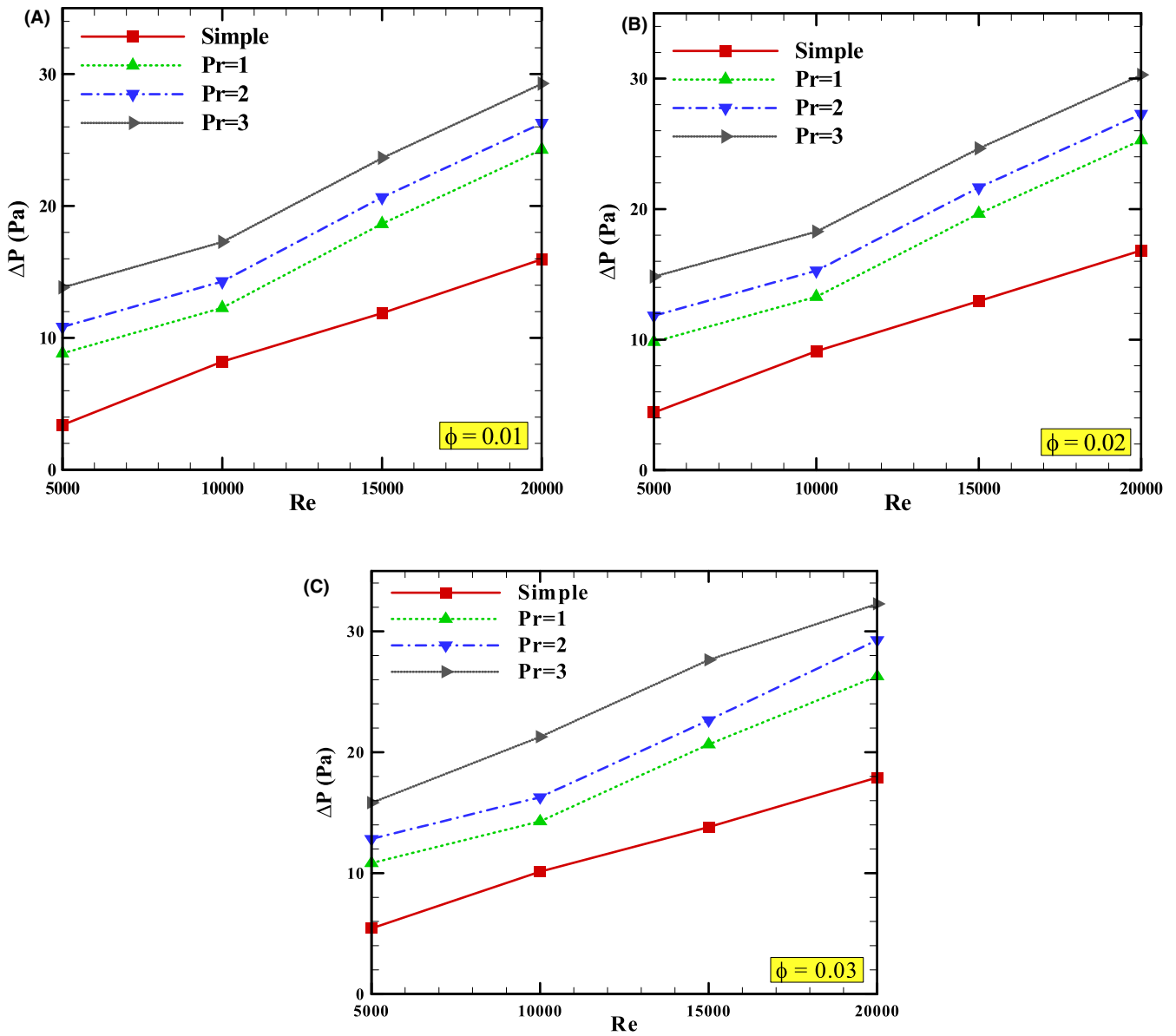


FIGURE 8 ΔP variations against Reynolds number in a P-SC with turbulator at different ROPs for (A) $\phi = 0.01$, (B) $\phi = 0.02$, and (C) $\phi = 0.03$

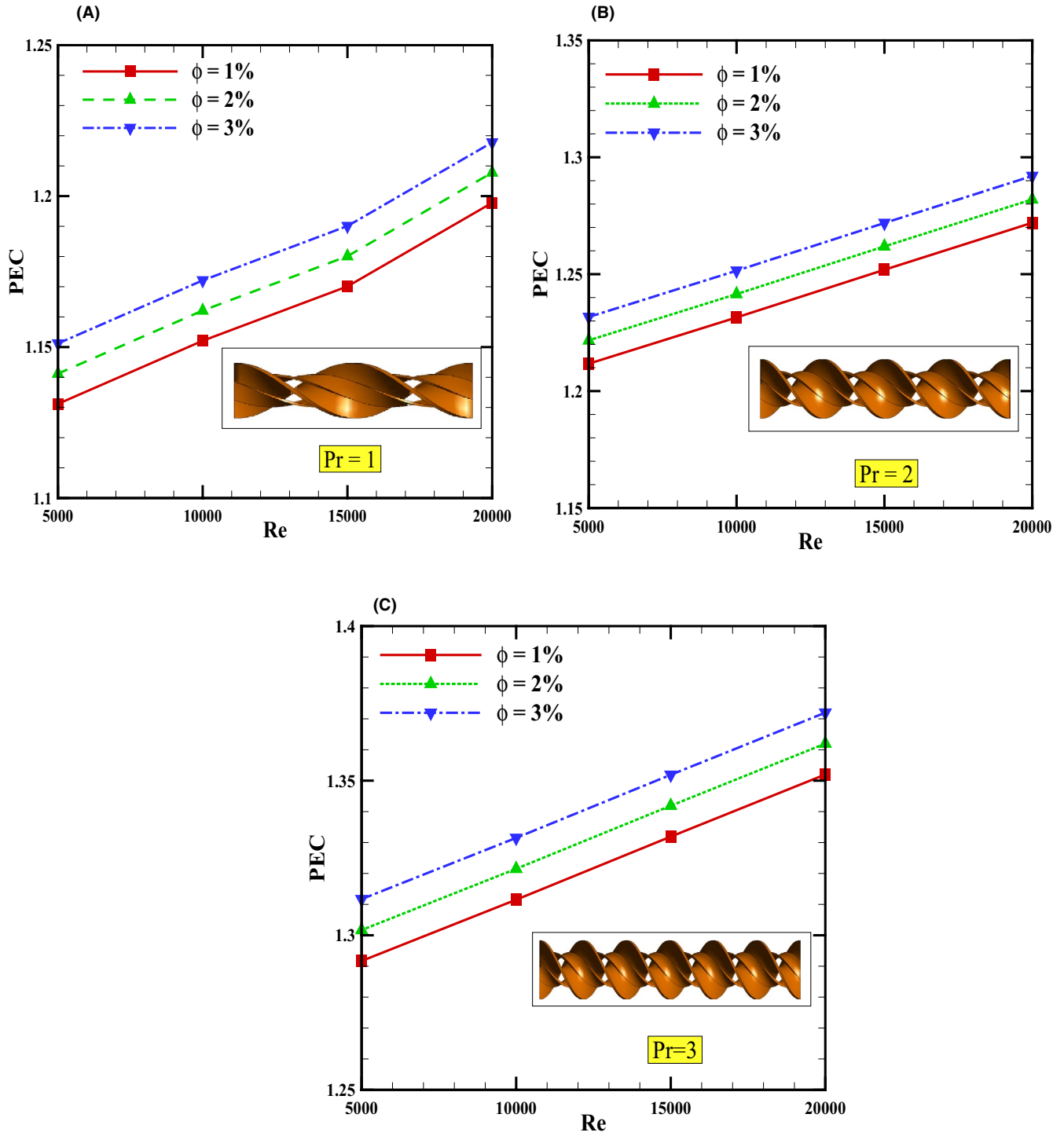


FIGURE 9 Changes of PEC index against Reynolds number in volume fractions of 1%-3% of nanoparticles in P-SC with combined turbulator for (A) ROP = 1, (B) ROP = 2, and (C) ROP = 3

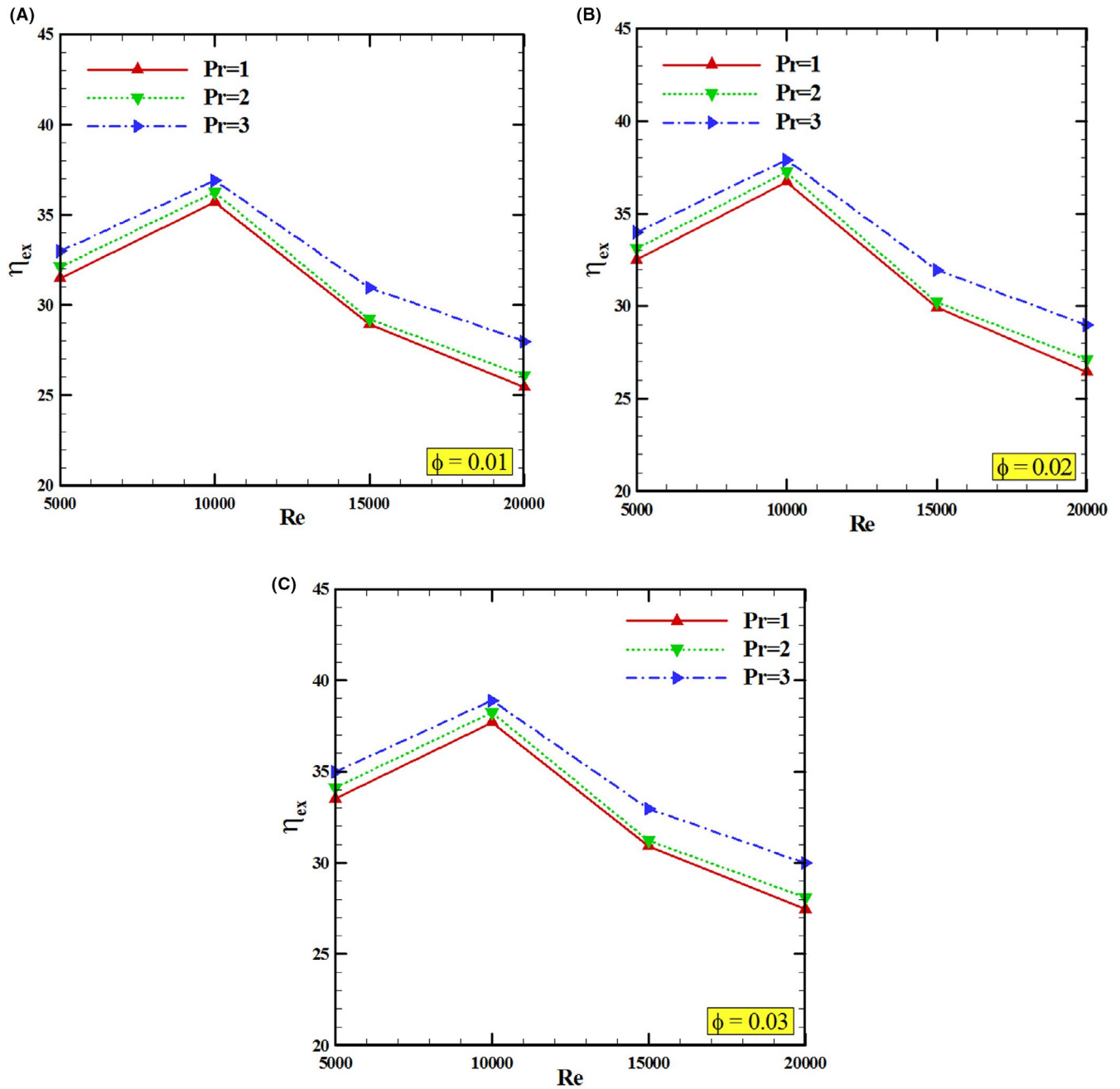


FIGURE 10 Exergy performance discrepancy against Re number in P-SC with compound turbulator for $ROP = 1, 2,$ and 3 in volume fractions of (A) $0.01,$ (B) $0.02,$ and (C) 0.03

ACKNOWLEDGEMENTS




This work was supported by the Taif University Researchers Supporting Project, Taif University, Taif, Saudi Arabia, under Project TURSP-2020/121.

NOMENCLATURE

ρ density (kg/m^3)
 cp specific heat capacity (J/kg.K)
 f friction coefficient (-)
 k thermal conductivity (W/m.K)
 Nu Nusselt number (-)

P pressure (Pa)
 Re Reynolds number (-)
 C velocity (m/s)
 HTR heat transfer rate
 ROP ratio of pitch
 PEC performance evaluation coefficient
 μ viscosity ($\text{N}\cdot\text{s/m}^2$)
 φ volume fraction
 η pump efficiency
 nf nanofluid
 np nanoparticle

ORCID

Ahmad Alahmadi  <https://orcid.org/0000-0002-1996-7671>
 Goshtasp Cheraghian  <https://orcid.org/0000-0002-0262-8374>
 Cornelius Siakachoma  <https://orcid.org/0000-0003-4854-5811>

REFERENCES

- Hajatzadeh Pordanjani A, Aghakhani S, Afrand M, Mahmoudi B, Mahian O, Wongwises S. An updated review on application of nanofluids in heat exchangers for saving energy. *Energy Convers Manag.* 2019;198:111886.
- Pordanjani AH, Aghakhani S, Afrand M, et al. Nanofluids: physical phenomena, applications in thermal systems and the environment effects- a critical review. *J Clean Prod.* 2021;2021:128573.
- Shahsavari A. Experimental evaluation of energy and exergy performance of a nanofluid-based photovoltaic/thermal system equipped with a sheet-and-sinusoidal serpentine tube collector. *J Clean Prod.* 2021;287:125064.
- Shahsavari A, Jha P, Arici M, Kefayati G. A comparative experimental investigation of energetic and exergetic performances of water/magnetite nanofluid-based photovoltaic/thermal system equipped with finned and unfinned collectors. *Energy.* 2021;220:119714.
- Shahsavari A, Jha P, Arici M, Estellé P. Experimental investigation of the usability of the rifled serpentine tube to improve energy and exergy performances of a nanofluid-based photovoltaic/thermal system. *Renew Energy.* 2021;170:410–425.
- Khanmohammadi S, Shahsavari A. Comparison of the performance of different designs of a combined system consisting of a photovoltaic thermal unit and a sensible rotary heat exchanger. *Sustain Energy Technol Assess.* 2021;45:101203.
- Rahmanian S, Rahmanian-Koushkaki H, Omidvar P, Shahsavari A. Nanofluid-PCM heat sink for building integrated concentrated photovoltaic with thermal energy storage and recovery capability. *Sustain Energy Technol Assess.* 2021;46:101223.
- Xiong Q, Altnji S, Tayebi T, et al. A comprehensive review on the application of hybrid nanofluids in solar energy collectors. *Sustain Energy Technol Assess.* 2021;47:101341.
- Moravej M, Doranehgard MH, Razeghizadeh A, et al. Experimental study of a hemispherical three-dimensional solar collector operating with silver-water nanofluid. *Sustain Energy Technol Assess.* 2021;44:101043.
- Rahmani E, Moradi T, Fattahi A, et al. Numerical simulation of a solar air heater equipped with wavy and raccoon-shaped fins: the effect of fins' height. *Sustain Energy Technol Assess.* 2021;45:101227.
- Hazra SK, Michael M, Nandi TK. Investigations on optical and photo-thermal conversion characteristics of BN-EG and BN/CB-EG hybrid nanofluids for applications in direct absorption solar collectors. *Sol Energy Mater Sol Cells.* 2021;230:111245.
- Fattahi A. On the rotary concentrated solar collector containing twisted ribs and MgO-Ag-water nanofluid. *J Taiwan Inst Chem Eng.* 2021;124:29–40.
- Yan S-R, Aghakhani S, Karimipour A. Influence of a membrane on nanofluid heat transfer and irreversibilities inside a cavity with two constant-temperature semicircular sources on the lower wall: applicable to solar collectors. *Phys Scr.* 2020;95(8):085702.
- Shahsavari A, Talebizadeh P, Tabaei H. Optimization with genetic algorithm of a PV/T air collector with natural air flow and a case study. *J Renew Sustain Energy.* 2013;5(2):023118. <https://doi.org/10.1063/1.4798312>
- Sari-Ali I, Rahmoun K, Chikh-Bled B, et al. Mono-crystalline silicon photovoltaic cells under different solar irradiation levels. *Optik.* 2020;223:165653.
- Nikzad A, Chahartaghi M, Ahmadi MH. Technical, economic, and environmental modeling of solar water pump for irrigation of rice in Mazandaran province in Iran: a case study. *J Clean Prod.* 2019;239:118007.
- Ahmadi MH, Mehrpooya M. Thermo-economic modeling and optimization of an irreversible solar-driven heat engine. *Energy Convers Manage.* 2015;103:616–622.
- Abbasipour B, Niroumand B, Monir Vaghefi SM, Abedi M. Tribological behavior of A356–CNT nanocomposites fabricated by various casting techniques. *Trans Nonferrous Metals Soc China.* 2019;29(10):1993–2004.
- Abedi M, Moskovskikh DO, Mukasyan AS. *Reactive Flash Spark Plasma Sintering of Alumina Reinforced by Silicon Carbide Nanocomposites: Physicochemical Study*, in International Symposium on Self-Propagating High-Temperature Synthesis, (XV), Moscow, Russia, 2019, pp. 10–11.
- Abedi M, Moskovskikh DO, Rogachev AS, Mukasyan AS. Spark plasma sintering of titanium spherical particles. *Metall Mater Trans B.* 2016;47(5):2725–2731.
- Keyvani N, Azarniya A, Hosseini HRM, Abedi M, Moskovskikh D. Thermal stability and strain sensitivity of nanostructured aluminum titanate (Al₂TiO₅). *Mat Chem Phys.* 2019;223:202–208.
- Kuskov KV, Abedi M, Moskovskikh DO, Serhienko I, Mukasyan AS. Comparison of conventional and flash spark plasma sintering of Cu–Cr pseudo-alloys: kinetics. *Struct Prop Metals.* 2021;11(1):141.
- Torosyan KS, Sedegov AS, Kuskov KV, et al. Reactive, nonreactive, and flash spark plasma sintering of Al₂O₃/SiC composites—A comparative study. *J Am Ceramic Soc.* 2020;103(1):520–530.
- Ibrahim M, Saeed T, Chu Y-M, Ali HM, Cheraghian G, Kalbasi R. Comprehensive study concerned graphene nano-sheets dispersed in ethylene glycol: experimental study and theoretical prediction of thermal conductivity. *Powder Technol.* 2021;386:51–59.
- Wei H, Afrand M, Kalbasi R, Ali HM, Heidarshenas B, Rostami S. The effect of tungsten trioxide nanoparticles on the thermal conductivity of ethylene glycol under different sonication durations: an experimental examination. *Powder Technol.* 2020;374:462–469.
- Tian X-X, Kalbasi R, Qi C, Karimipour A, Huang H-L. Efficacy of hybrid nano-powder presence on the thermal conductivity of the engine oil: an experimental study. *Powder Technol.* 2020;369:261–269.
- Rostami S, Kalbasi R, Talebkeikhah M, Goldanlou AS. Improving the thermal conductivity of ethylene glycol by addition of hybrid nano-materials containing multi-walled carbon nanotubes and titanium dioxide: applicable for cooling and heating. *J Therm Anal Calorim.* 2021;143(2):1701–1712.
- Tian M-W, Rostami S, Aghakhani S, Goldanlou AS, Qi C. A techno-economic investigation of 2D and 3D configurations of fins and their effects on heat sink efficiency of MHD hybrid nanofluid with slip and non-slip flow. *Int J Mech Sci.* 2021;189:105975.

29. Bahrami D, Nadooshan AA, Bayareh M. Numerical study on the effect of planar normal and Halbach magnet arrays on micromixing. *Int J Chem React Eng.* 2020;18(9):20200080. <https://doi.org/10.1515/ijcre-2020-0080>
30. Nguyen Q, Bahrami D, Kalbasi R, Karimipour A. Functionalized Multi-Walled carbon Nano Tubes nanoparticles dispersed in water through an Magneto Hydro Dynamic nonsmooth duct equipped with sinusoidal-wavy wall: Diminishing vortex intensity via nonlinear Navier-Stokes equations. *Math Methods Appl Sci.* 2020. In Press. <https://doi.org/10.1002/mma.6528>
31. Wole-Osho I, Okonkwo EC, Abbasoglu S, Kavaz D. nanofluids in solar thermal collectors: review and limitations. *Int J Thermophys.* 2020;41(11):1–74.
32. Ranjbarzadeh R, Akhgar A, Musivand S, Afrand M. Effects of graphene oxide-silicon oxide hybrid nanomaterials on rheological behavior of water at various time durations and temperatures: synthesis, preparation and stability. *Powder Technol.* 2018;335:375–387.
33. Karimipour A, Bahrami D, Kalbasi R, Marjani A. Diminishing vortex intensity and improving heat transfer by applying magnetic field on an injectable slip microchannel containing FMWNT/water nanofluid. *J Therm Anal Calorim.* 2021;144(6):2235–2246.
34. Razavi SE, Farhangmehr V, Babaie Z. Numerical investigation of hemodynamic performance of a stent in the main branch of a coronary artery bifurcation. *BioImpacts.* 2019;9(2):97.
35. Afrand M, Farahat S, Nezhad AH, Ali Sheikhzadeh G, Sarhaddi F. 3-D numerical investigation of natural convection in a tilted cylindrical annulus containing molten potassium and controlling it using various magnetic fields. *Int J Appl Electromagn Mechanics.* 2014;46:809–821.
36. Aghakhani S, Pordanjani AH, Karimipour A, Abdollahi A, Afrand M. Numerical investigation of heat transfer in a power-law non-Newtonian fluid in a C-Shaped cavity with magnetic field effect using finite difference lattice Boltzmann method. *Comput Fluids.* 2018;176:51–67.
37. Shiriny A, Bayareh M, Nadooshan AA, Bahrami D. Forced convection heat transfer of water/FMWNT nanofluid in a microchannel with triangular ribs. *SN Appl Sci.* 2019;1(12):1–11.
38. Dinarvand M, Abolhasani M, Hormozi F, Bahrami Z. Cooling capacity of magnetic nanofluid in presence of magnetic field based on first and second laws of thermodynamics analysis. *Energy Sources, Part A: Recovery, Utili, Environ Eff.* 2021. In Press. <https://doi.org/10.1080/15567036.2021.1872746>
39. Shiriny A, Bayareh M. Inertial focusing of CTCs in a novel spiral microchannel. *Chem Eng Sci.* 2021;229:116102.
40. Pordanjani AH, Aghakhani S. Numerical investigation of natural convection and irreversibilities between two inclined concentric cylinders in presence of uniform magnetic field and radiation. *Heat Transfer Eng.* 2021. In Press. <https://doi.org/10.1080/01457632.2021.1919973>
41. Sheikholeslami M, Jafaryar M, Abohamzeh E, Shafee A, Babazadeh H. Energy and entropy evaluation and two-phase simulation of nanoparticles within a solar unit with impose of new turbulator. *Sustain Energy Technol Assess.* 2020;39:100727.
42. Akbarzadeh S, Valipour MS. The thermo-hydraulic performance of a parabolic trough collector with helically corrugated tube. *Sustain Energy Technol Assess.* 2021;44:101013.
43. Hassan H, Yousef MS, Abo-Elfadl S. Energy, exergy, economic and environmental assessment of double pass V-corrugated-perforated finned solar air heater at different air mass ratios. *Sustain Energy Technol Assess.* 2021;43:100936.
44. Ahmed HE, Ahmed MI, Yusoff MZ. Heat transfer enhancement in a triangular duct using compound nanofluids and turbulators. *Appl Therm Eng.* 2015;91:191–201.
45. Akbari OA, Toghraie D, Karimipour A, et al. Investigation of rib's height effect on heat transfer and flow parameters of laminar water–Al₂O₃ nanofluid in a rib-microchannel. *Appl Math Comput.* 2016;290:135–153.
46. Amirahmadi S, Rashidi S, Abolfazli Esfahani J. Minimization of exergy losses in a trapezoidal duct with turbulator, roughness and beveled corners. *Appl Therm Eng.* 2016;107:533–543.
47. Sheikholeslami M, Ganji DD. Heat transfer improvement in a double pipe heat exchanger by means of perforated turbulators. *Energy Convers Manage.* 2016/11/01/, 2016.;127:112–123.
48. Sheikholeslami M, Ganji DD. Heat transfer enhancement in an air to water heat exchanger with discontinuous helical turbulators; experimental and numerical studies. *Energy.* 2016;116:341–352.
49. Ma Y, Mohebbi R, Rashidi M, Yang Z. Study of nanofluid forced convection heat transfer in a bent channel by means of lattice Boltzmann method. *Phys Fluids.* 2018;30(3):032001. <https://doi.org/10.1063/1.5022060>
50. Eiamsa-ard S, Wongcharee K. Convective heat transfer enhancement using Ag-water nanofluid in a micro-fin tube combined with non-uniform twisted tape. *Int o Mech Sci.* 2018;146–147:337–354.
51. Akbarzadeh M, Rashidi S, Karimi N, Ellahi R. Convection of heat and thermodynamic irreversibilities in two-phase, turbulent nanofluid flows in solar heaters by corrugated absorber plates. *Adv Powder Technol.* 2018;29(9):2243–2254.
52. Sharafeldin MA, Gróf G. Evacuated tube solar collector performance using CeO₂/water nanofluid. *J Clean Prod.* 2018;185:347–356.
53. Bahrami D, Abbasian-Naghneh S, Karimipour A, Karimipour A. Efficacy of injectable rib height on the heat transfer and entropy generation in the microchannel by affecting slip flow. *Math Methods Appl Sci.* 2020. In Press. <https://doi.org/10.1002/mma.6728>
54. Subramani J, Nagarajan PK, Mahian O, Sathyamurthy R. Efficiency and heat transfer improvements in a parabolic trough solar collector using TiO₂ nanofluids under turbulent flow regime. *Renew Energy.* 2018;119:19–31.
55. Bazdidi-Tehrani F, Khabazipur A, Vasefi SI. Flow and heat transfer analysis of TiO₂/water nanofluid in a ribbed flat-plate solar collector. *Renew Energy.* 2018;122:406–418.
56. Nguyen Q, Bahrami D, Kalbasi R, Bach QV. Nanofluid flow through microchannel with a triangular corrugated wall: heat transfer enhancement against entropy generation intensification. *Math Methods Appl Sci.* 2020. In Press. <https://doi.org/10.1002/mma.6705>
57. Obaid ZAH, Al-damook A, Khalil WH. The thermal and economic characteristics of solar air collectors with different delta turbulators arrangement. *Heat Transf—Asian Res.* 2019;48(6):2082–2104.
58. Singh AP, Akshayveer A, Kumar O, Singh P. Efficient design of curved solar air heater integrated with semi-down turbulators. *Int J Therm Sci.* 2020;152:106304.
59. Ekiciler R, Arslan K, Turgut O, Kurşun B. Effect of hybrid nanofluid on heat transfer performance of parabolic trough solar collector receiver. *J Therm Anal Calorim.* 2021;143(2):1637–1654.

60. Sheikholeslami M, Farshad SA. Nanoparticle transportation inside a tube with quad-channel tapes involving solar radiation. *Powder Technol.* 2021;378:145–159.
61. Sadripour S, Chamkha AJ. The effect of nanoparticle morphology on heat transfer and entropy generation of supported nanofluids in a heat sink solar collector. *Therm Sci Eng Prog.* 2019;9:266–280.
62. Rostami S, Aghakhani S, Hajatzadeh Pordanjani A, et al. A review on the control parameters of natural convection in different shaped cavities with and without nanofluid. *Processes.* 2020;8(9):1011.
63. Shahsavar Goldanlou A, Sepehrirad M, Dezfulizadeh A, Golzar A, Badri M, Rostami S. Effects of using ferromagnetic hybrid nanofluid in an evacuated sweep-shape solar receiver. *J Therm Anal Calorim.* 2021;143(2):1623–1636.
64. Aghaei A, Khorasanizadeh H, Sheikhzadeh GA. A numerical study of the effect of the magnetic field on turbulent fluid flow, heat transfer and entropy generation of hybrid nanofluid in a trapezoidal enclosure. *Eur Phys J Plus.* 2019;134(6):310.
65. Molana M, Dogonchi AS, Armaghani T, Chamkha AJ, Ganji DD, Tlili I. Investigation of hydrothermal behavior of Fe_3O_4 - H_2O nanofluid natural convection in a novel shape of porous cavity subjected to magnetic field Dependent (MFD) viscosity. *J Energy Storage.* 2020;30:101395.
66. He W, Toghraie D, Lotfipour A, Pourfattah F, Karimipour A, Afrand M. Effect of twisted-tape inserts and nanofluid on flow field and heat transfer characteristics in a tube. *Int Commun Heat Mass Transfer.* 2020;110:104440.

How to cite this article: Khetib Y, Alahmadi A, Alzaed A, Sharifpur M, Cheraghian G, Siakachoma C. Simulation of a parabolic trough solar collector containing hybrid nanofluid and equipped with compound turbulator to evaluate exergy efficacy and thermal-hydraulic performance. *Energy Sci Eng.* 2021;00:1–14. <https://doi.org/10.1002/ese3.975>